A Trade-Off Analysis of Adaptive and Non-Adaptive Future Optimized Rule Curves Based on Simulation Algorithm

Mahnoosh Moghaddasi (mah_moghaddasi@hotmail.com)
Arak University
Sedigheh Anvari
Graduate University of Advanced Technology
Najmeh Akhondi
Arak University

Research Article

Keywords: Climate change, hedging rules, optimization, Zarrineh Rud, simulation,adaptive

Posted Date: June 29th, 2021

DOI: https://doi.org/10.21203/rs.3.rs-615841/v1

A trade-off analysis of adaptive and non-adaptive future optimized rule curves based on simulation algorithm

Mahnoosh Moghaddasi[1,2], Sedigheh Anvari[3], Najemeh Akhondi[4]

[1]Associate professor, Department of Water Resources, Faculty of Agriculture and Environment, Arak University, Arak, Iran.
[2]Associate professor, Department of Water Resources, Water Institute, Arak University, Arak, Iran.

[3]Assistant Professor, Department of Ecology, Institute of Science and High Technology and Environmental Science, Graduate University of Advanced Technology, Kerman, Iran.

[4]Master student of irrigation and drainage, Department of Water Resources, Faculty of Agriculture and Environment, Arak University, Arak, Iran.

Corresponding author:Mahnoosh Moghaddasi
Corresponding email : mah_moghaddasi@hotmail.com , m-moghaddasi@araku.ac.ir
Telefax: +988632623702

Abstract

This study aims to investigate the performance of Zarrineh Rud reservoir by implementing strategies for adaptation to climate change. Using sequent peak algorithm (SPA), the rule curve were simulated. Then, the optimal rule curve was procured through GA-SPA, aiming to minimize the water shortage. The future data were downscaled using SDSM based on CanEsm2 model and under RCP2.6 and RCP8.5. Finally, in view of environmental demand, reservoir performance indices were calculated for both non-adaptive and adaptive policies during all future periods (2020-2076). Results showed simulation with the static hedging rules managed to significantly reduce the average vulnerability index (by 60%) compared to no hedging, while the dynamic hedging rules outperformed static hedging rules only by 9%. Therefore, considering the insignificant improvement in reservoir performance using dynamic rules and their complexity, static hedging rules are recommended as the better option for adaptation during climate change.

Keywords: Climate change, hedging rules, optimization, Zarrineh Rud, simulation,adaptive

1. Introduction

Surface water reservoirs play an important role in water supply in many countries across the world. In an arid country like Iran, more than 90% of renewable water is consumed by the agricultural sector, which is mostly supplied by surface water reservoirs (Anvari et al., 2017). These reservoirs must be designed such that they can retain the excess wet season runoff for dry or low-precipitation periods, and provide adequate dam release to meet downstream demands (Guo et al., 2004; Chen et al., 2007; Compos, 2010; Anvari et al., 2019). The best option here is a design based on the historical inflow. However, this can cause problems if there is a change in the stream flow due to climate change (IPCC, 2007).

Most of these reservoirs are operated using a standard operating policy (SOP) based on the water available at the beginning of each month (initial reservoir storage plus inflow) (Yin et al., 2015). Although these rule curves are easy to use, they can cause a greater vulnerability and higher water shortage in the reservoir under climate change. To reduce there impacts, hegding (or water rationary) during normal operational periods is carried out (Bhatia et al., 2018; Tu et al., 2008; Eum et al., 2011; Srinivasan and Kumar, 2018; Chang et al., 2019).Therefore, many studies have focused on evaluating the impact of climate change on reservoir performance in order to adapt to and reduce these effect (Fowler et al., 2003; Nawaz & Adeloye, 2006; Li et al., 2009; Moghaddasi, et al., 2010, Traynham et al., 2011; Adeloye et al., 2013; Hernandez et al.,2017; Mushtagh & Moghaddasi, 2017; Ehteram et al., 2018). Most studies indicate a climate change-induced deterioration of reservoir performance involving reduced reliability and increased water shortage, although there is still uncertainty regarding these effects (Soundharajan, et al., 2016; Kermani et al., 2020). Such adverse conditions need further adaptation and mitigation. Several studies have focused on this topic, some of which are reviewed below. Raje and Mujumdar (2010) examined the impact of climate change on the performance of the Hirakud multipurpose reservoir in India. Their results showed that SOP could decrease the reliability index and increase vulnerability. Then, a stochastic dynamics programming (SDP) model was developed accounting for inflow uncertainty to derive standard operating procedures, aiming to maximize the level of reliability. Compared to SOP, reservoir performance using this model showed a decrease in hydropower generation and increase in irrigation reliability, while its performance remained the same for flood control. Ashofteh and Haddad (2015) extracted an optimal operation policy for Aydughmush reservoir in East Azarbaijan, Iran during current and climate change conditions aiming to minimize vulnerability and maximize reliability using a multi-objective genetic programming (MO-GP) algorithm. The range of variations under current and climate change conditions were respectively 16-41% and 11-35% for the vulnerability index and 46-78% and 30-77% for the reliability index. Soundharajan et al. (2016) examined the performance of the Indian Pong Reservoir using modified SPA (MSPA) under climate change conditions. They first simulated the reservoir inflow through the HYSIM model. Based on the model output, 1000 synthetic datasets were generated using the Thomas-Firing method, and then the optimal reservoir rule curve was determined using MSPA and GA. Results demonstrated that the reservoir capacity would be reduced in the future with a 0.3 coefficient of variation. The coefficient of variation was the highest for the vulnerability index at 0.5 and the lowest for the reliability index. Adeloye et al. (2016) explored the impact of Hedging-Integrated rule curves on the performance of the Indian Pong reservoir under current and future conditions. Using SPA, they first designed the reservoir and simulated the rule curve. Then, the rule curve was calculated using hedging rules and GA aiming to minimize the water shortage. In conclusion, they reduced the vulnerability index from 61% to 20%. Prasanchum and Kangrang (2017) used a GA-connected reservoir simulation model to search for optimal rule curves over a 50-year

period (2014-2064) in the Lampao reservoir, in northeastern Thailand. The impact of climate change was simulated using PRECIS under A2 and B2 emission scenarios, and the future land use maps were created using the CA Markov model. Furthermore, using a SWAT hydrological model, the future inflow to the reservoir was assessed. As a result, the new rule curves and their performance indices were improved, reducing the frequency of water shortage even in the situation where irrigation areas were expanded. Esa Kia (2018) investigated the impact of climate change on the reliability of water supply downstream of Haraz reservoir using the CanESM2 model under RCP2.6 and RCP8.5 scenarios. The optimal operating policy was developed to minimize the sum square of relative deficiency using Firefly Algorithm (FA) and GA during the operation period. The results showed that under current conditions, the FA method, with an 88.3% water supply reliability, outperformed GA (82.4%) and SOP (66.7%), meeting the downstream demand. Under the climate change conditions, it showed lower time and volume-based reliability, and higher vulnerability and water shortage indices. Adeloye and Dau (2019) studied the performance of the Indian Pong reservoir using static and dynamic hedging rules under climate change conditions. According to their results, static hedging rules were effective in reducing vulnerability (from over 60% to less than 25%), but the volume-based reliability remained the same. The dynamic hedging rules slightly improved the values of these indicators, however, considering their complexity, static rules seem to be more efficient. In another study, the modified linear decision rule (MLDR) operation policy was adopted to reduce the impact of climate change on reservoir operation. The findings indicated that the presence of enough water (optimistic scenario) is necessary for the optimal performance of SOP, otherwise (pessimistic scenarios) operating SOP would not be able to properly supply drinking water, resulting in a crisis. On the other hand, the MLDR policy does not allow for the complete draining of the reservoir, reducing the period in which the reservoir remains empty by over 90% in all future water demand scenarios as compared to SOP (Alimohammadi et al., 2020). The present study to analyze the rule curve of Zarrineh Rud reservoir under climate change conditions. First, the rule curve was developed based on historical conditions and using SPA, which was then optimized through GA-SPA. Given the optimal rule curve and the inflow under climate change conditions (CanEsm2 model and RCP2.6 and RCP 8.5 scenarios), reservoir performance indices in non-adaptive policies were calculated for three future periods. Since the GA-SPA curve meets the full demands for adaptation to climate change conditions, middle conditions were extracted to meet the amount of the full demands through static and dynamic hedging rules, i.e. critical rule curve (CRC) (adaptive). Finally, reservoir performance was evaluated and compared considering the environmental demand for both non-adaptive and adaptive politics.

2. Case Study

Zarrineh Rud is the most important catchment of the Lake Urmia (LU), providing over 40% of the total annual inflow into the LU basin. The catchment is located at 45◦47' to 47◦20' N and 35◦41' to 37◦27' E (Figure 1). The total area of the basin is about 12,025 km^2, and the length of its main channel is 300 km. The average annual rainfall in the basin is 390 mm. The Zarrineh Rud reservoir is the only dam in the basin, and it is operated for agricultural and drinking water demands (Table 1). This dam has a storage capacity of 760 MCM and its active storage is 654 MCM. Meteorological and hydrometric input data for 1990-2016 period were collected from the Iranian Meteorological Organization (IMO) and the Ministry of Energy for two synoptic stations (Saghaz and Takab) and one hydrometric station (upstream of the dam). In addition, future climate data were projected based on CanEsm2 model from AR5 for near future (2020-2038), middle future (2039-2057), and far future (2058-2076) using future climate scenarios: RCP2.6 and RCP8.5. It should be noted that the amount of downstream agricultural demand was obtained from Ahmadzadeh et al. (2016) and environmental demand from Abdi et al. (2014) (Table 2).

Figure 1.

Table 1.

Table 2.

3. Methodology

The general research flowchart is presented in Figure 2 for a better understanding of the research methodology. The methods are explained in more detail below.

3.1. Statistical DownScaling Model (SDSM Model)

In order to produce precipitation and temperature data, the data of CanESM2 model were downscaled using SDSM. This model has three scenarios: RCP2.6, RCP4.5, and RCP8.5. SDSM is used to create a quantitative relationship between large-scale variables in the general circulation models (GCMs) and small-scale variables (local/regional scale) (Wilby et al., 2002). The method consists of four main parts, which include determination of the NCEP predictor variables, model calibration, model verification, and finally simulation of precipitation and temperature data under the RCP scenarios for the future period.

Figure 2.

3.2. HBV-light Model

The HBV model is a semi-distributed conceptual rainfall-runoff model. It simulates stream flow using rainfall, temperature, and potential evapotranspiration (PET) as input (Bergström 1976, 1995; Seibert, 1997). The model is subdivided into three routines; snow and glacier routine, soil moisture routine, and runoff generation routine (Figure. 3). The degree-day

method at five elevation zones of roughly 500 m intervals was used to calculate the snow accumulation and melt. This temperature-based approach is practical since, unlike physically-based energy balance modeling, the HBV-light model does not require comprehensive datasets for the upstream high altitudes (including climate, snow depth, or snow water equivalent data) to spatially distribute the climate variables. Meanwhile, in the soil moisture routine, groundwater recharge and actual evapotranspiration are functions of water storage. Finally, recharge is transformed into discharge through the lumped response function. See Seibert and Vis (2012) for a detailed description of the model.

Figure 3.

3.3. Sequent Peak Algorithm (SPA)

Graphical mass curve provides an easy way to obtain the failure-free capacity estimate (Ripple, 1883), however, it is not a fully suitable method due to its graphical implementation, especially for repeated analyses required for the Monte Carlo simulation. On the other hand, generation of non-unique outcome and the iterative nature of behavior simulation makes it inefficient for failure-free capacity estimation (see Adeloye et al., 2001), and it may also misbehave (Pretto et al., 1997). Therefore, a sequent peak algorithm (SPA) was used to estimate the required failure-free reservoir capacity, which does not suffer from these limitations (McMahon & Adeloye, 2005):

$$K_{t+1} = max(0, K_t + D_t - Q_t) \quad (1)$$

$$K_a = \max(K_{t+1}) \quad (2)$$

where K $_a$is reservoir capacity, K_{t+1} and K_t are respectively the sequential deficits at the end and the start of time period t, D_t is the demand during t, Q_t is the inflow during t, and N is the number of months in the data record. As a critical period reservoir sizing technique, SPA assumes that the reservoir is full at the start and the end of the cycle similar to other sizing techniques, i.e. $K_0 = K_N = 0$. When this is not the case, i.e. $K_N = 0$, the SPA cycle is repeated by setting the initial deficit to K_N, i.e. $K_0 = K_N$. This second iteration should end with K_N unless the demand is higher than the mean annual runoff. SPA, however, does not need to assume that the reservoir is initially full, since this will become clear during the first cycle if this assumption is not valid, and amended during the second cycle.

3.4. Reservoir Behavior Simulation

Behavior simulation was carried out using the following relations to assess the performance of the historical reservoir capacity and operational rule curves (McMahon & Adeloye, 2005):

(3)

$$S_t = K_a - K_t$$

$$URC_m = \max(S_{y,m}),\ y = 1,n \quad m = \quad (4)$$

1,12

$$LRC_m = \min(S_{y,m}),\ y = 1,n \quad m = \quad (5)$$

1,12

$$S_{y,m} = S_{12(y-1)+m} \quad (6)$$

$$t = \quad (7)$$

$$12(y-1)+m$$

$$S_{t+1} = S_t + Q_t + \acute{D}_t - E_t \qquad LRC_m \leq S_{t+1} \leq URC_m \quad (8)$$

where S_{t+1} and $S_t$are respectively, reservoir storage at the end and beginning of the time period t; D_t is the actual water released during t (which may be different from the demand D_t, depending on the operating rule curves); LRC is the lower rule curve ordinate for the month corresponding to t; and, URC is the corresponding upper rule curve ordinate. Generally, there are several aspects to the failures in the operation of a reservoir including extent, number, and severity (Jain, 2010). Indicators such as reliability, resiliency, and vulnerability show these aspects as explained in the following (Hashimoto et al., 1982):

Reliability

Water supply reliability is the probability that the available water supply meets the water demand during the simulation period. Two indices are generally followed in reservoir regulation. One of them is time-based reliability that is estimated as:

$$Rel_t = Ns/N \quad (9)$$

where Rel_t is time-based reliability and $N_s$is the total number of intervals (months) out of N (months) in which the demand was met. Another one is volume-based reliability that is expressed as:

$$Rel_v = Vs/Vd \tag{10}$$

where Rel_v is volume-based reliability, V_s is the volume of water supplied, and V_d is the volume of water demanded during a given period.

Vulnerability

Vulnerability expresses the severity of failures. The definition of vulnerability used here is the average period shortfall as a ratio of the average period demand (Sandoval-Soils et al., 2011).

$$Vul = \frac{\sum_{t=1}^{f_d} \frac{D_t - D't}{D_t}}{f_d} \tag{11}$$

where Vul is vulnerability and D'_t is the actual release during t.

3.5. Genetic Algorithm

GA as an optimal search engine has been successfully employed in a variety of water resource management problems over the years. It is based the on survival-of-the-fitness principle and contains three main types of operators including selection, crossover, and mutation. Similar to other optimization algorithms, GA begins with the definitions of the objective function and decision variables, then utilizes the following set of instructions, and finally ends by testing for convergence (Goldberg, 1998; Kacprzyk, 2006; Castillo et al., 2014).

1. Start with an initial population that is randomly generated using n chromosomes, known as a set of suitable solutions to the problem.
2. Compute the fitness values of each individual chromosome in the population.
3. Repeat the steps below until creating an offspring:
   (a) Select a pair of parent chromosomes based on the fitness scores. The probability in which an individual chromosome is selected is usually a function of fitness.
   (b) Select a probability of crossover rate (Pc) to crossover the pair at a random point to make two separate offspring.
   (c) Select a probability of mutation (Pm) to mutate the mentioned two offspring and then put the resulting chromosome in the population.
4. Replace this population with the newly generated population.
5. Go to step 2.

In this research, the objective (or fitness) function adopted for the GA optimization to develop the basic rule curves was:

$$Minimise \ \sum_{i=1}^{N}(D_t - D_t')^2 \qquad t \in N \tag{12}$$

The constraints are as follows:

$$S_{t+1} = S_t + Q_t - D_t - E_t \quad LRC_m \leq S_{t+1} \leq URC_m \tag{13}$$

$$WA_t = S_t + Q_t \tag{14}$$

$$if\ WA_t \geq LRC_m \qquad D'_t = S_t + Q_t - E_t - URC_m \ \&\ ER_t = D'_t - D_t \tag{15}$$

$$if\ URC_m \geq WA_t \geq LRC_m \quad D'_t = D_t \quad \& \quad ER_t = 0 \tag{16}$$

$$if\ WA_t \leq LRC_m \quad D'_t = 0 \tag{17}$$

where WA_t is the water available at the beginning of time period (month) t; ER_t is the excess release during time period t, St is the storage at the beginning of t, D'_t is the actual release, m is the month of the year and is related to the year y and simulation period t, E_t is net evaporation (ignored), and all other symbols are as previously defined. The constraint on the right-hand side of Eq. (13) limits the available water in any given month to the interval $[LRC_m, URC_m]$. The decision variables for the optimization are URC_m and LRC_m; m=1..,12 ordinates for each month m of the year, giving a total of 24 variables, including 12 values representing the 12 monthly ordinates for URC and 12 values representing the monthly ordinates for the LRC.

Figure 4.

3.6. Hedging Rules for Adaptive Policy

One method to improve the water shortages is to hedge or save some of the water during normal operation, i.e., when the reservoir state is in the interval [LRC_m, URC_m], and use the saved water during later dry periods. The timing and amount of the hedging are achieved using a CRC that lies between LRC and URC. The CRC thus represents the timing of hedging or saving. To derive hedging rule curves (static and dynamic), a GA optimization model is developed with the same objective function used for optimizing the main rule curves (see Eq. (12)) and its constraint is as follows:

$$if \quad URC_m \geq WA_t \geq CRC_m, \quad D'_t = D_t, \quad R_t = 0 \tag{18}$$

$$if \quad CRC_m \geq WA_t \geq LRC_m, \quad D'_t = \alpha D_t, \quad ER_t = 0 \tag{19}$$

$$if \quad WA_t \leq LRC_m, \quad D'_t = 0 \tag{20}$$

$$if \quad 1 \geq \alpha \geq 0, \quad URC_m \geq CRC_m \geq LRC_m \tag{21}$$

$$if \quad 1 \geq \alpha_m \geq 0, \quad URC_m \geq CRC_m \geq LRC_m \tag{22}$$

where, CRCm is the critical rule curve ordinate for month m (=1, 2,…,12); α is the static rationing ratio, and α_m represents the dynamic rationing ratios (m=1,2,…12). All other variables are as defined previously.

3.7. Evaluation Criteria

Criteria such as the coefficient of determination (R^2), root mean square error (RMSE), mean absolute error (MAE), and mean bias error (MBE) were used for data analysis and model evaluation. Their relationships are presented below:

$$\mathrm{RMSE} = \sqrt{\frac{\sum_{m=1}^{n}(X_p - X_0)^2}{n}} \tag{23}$$

$$R^2 = \left[\frac{\frac{1}{n}\sum_{m=1}^{n}(X_p - \mu_0)(X_p - \mu_0)}{\sigma_{Xp} \times \sigma_{X0}}\right]^2 \tag{24}$$

$$\mathrm{MAE} = \frac{\sum_{m=1}^{n}|X_p - X_0|}{n} \tag{25}$$

$$\mathrm{MBE} = \frac{\sum_{m=1}^{n}(X_P - X_0)}{n} \tag{26}$$

where X is the simulated data, μ average of data, σ the standard deviation, and n the number of data. Subscripts p and o represent the simulated data and observed data, respectively. R^2

represents the linear relationship between simulated and observed data, which is between 0 and 1. The closer to 1, R^2 represents a stronger linear relationship between the simulated and observed data.

4. Results and Discussion

4.1. SDSM Model

First, the relationship between the dependent variable of mean temperature and daily precipitation in selected stations and large-scale NCEP was investigated to determine the variables with the highest correlation (Table 3). The large-scale ncepp5_vgl, ncepp500gl, and ncepptempgl variables respectively show the highest correlation with precipitation and temperature in both stations. Then, the model was calibrated and validated based on these variables for the years 1987-1999 and 2000-2005 (Table 4). The highest correlation related to temperature, equal to 0.96 and 0.97 for NCEP and 0.92 and 0.93 for CanEsm2 in the calibration. These values were 0.94 and 0.92 for NCEP and 0.90 and 0.91 for CanEsm2 in Saghaz and Takab stations during the validation, respectively. The RMSE values in both predictors had the highest error for the precipitation variable, considering its complexity (compared to temperature). The MBE values showed the model's acceptable accuracy in predicting climatic parameters.

Table 3.

Table 4.

4.2. Future Climate Data

After evaluating the model, the climatic parameters of temperature and precipitation were generated in the selected stations for the near (2020-2038), middle (2039-2057), and far (2058-2076) future periods based on the global CanESM2 model for RCP2.6 and RCP8.5 scenarios (Figure 5). For example, in Saghaz station, there are no specific trends in the monthly precipitation variations in these three periods. In the near future, the largest decrease and increase occurred in January (17%) and November (40%) under the RCP 2.6 scenario, respectively. Meanwhile, in the RCP 8.5 scenario, the highest decrease occurred in December (24%) and in contrast, the largest increase was in November (15%) compared to the baseline. In the far future, March had the highest increase (64%) and April exhibited the highest decrease (37%) under the RCP 2.6 scenario. In the RCP 8.5 scenario, the highest increase and decrease occurred in February (34%) and April (28%), respectively. Still, the rising temperature can be seen in both stations and different periods. In the near, middle, and far future periods, the temperature has risen by 0.76°C, 2.14°C, 2.34°C under the RCP2.6 scenario and 0.73°C, 2.25°C, and 2.67°C under the RCP8.5 scenario, respectively.

The highest increase in temperature in the near future occurred in September (1.4°C) and the lowest in February (0.03°C) in the RCP2.6 scenario. In the far future, the highest increase occurred in April (5°C) and the lowest in July (0.5°C) in the RCP8.5 scenario.

Figure 5.

4.3. HBV-light Model Simulation

First, using the weighted average method, the daily precipitation and temperature data in Saghaz and Takab stations were calculated. Then, using monthly evapotranspiration, the daily temperature, and precipitation data, the inflow to Zarrineh Rud reservoir was simulated for 1987-2018. The model calibration and validation periods were respectively 22 years (2018-1997) and 10 years (1987-1996) (Table 5). The automatic GA was used for model calibration.

Table 5.

Figure 6.

As shown in Figure 6, even though the model has failed in some points to satisfactorily simulate the maximum and minimum values, the HBV model has performed acceptably in the calibration period (correlation coefficient of 0.6) and the validation period (correlation coefficient of 0.77) (Table 4). Subsequently, the basin runoff in the near, middle, and far future periods was calculated under RCP2.6 and RCP8.5 scenarios (Figure 7). The result showed a reduction in the annual runoff in all of these three periods compared to the baseline. Accordingly, the largest average annual runoff decrease was realized in the middle period in RCP8.5 (39%) and the lowest in the near future in RCP2.6 (23%).

Figure 7.

4.4. Reservoir Performance Indices for Future Situation

4.4.1. GA-SPA under Non-adaptive Policy

The reservoir was first designed based on SPA simulation to meet the drinking and agricultural demands. Then, the rule curve was developed. This simulated rule curve was then optimized through GA-SPA (Figure 8). As it can be seen, in both algorithms, the highest variation in the LRC of the curve occurred during May and December and the URC during November. Reservoir performance indices were calculated with environmental demand in both situations (Table 6). As expected, the mean annual deficit in the GA-SPA algorithm is reduced by 2.5% compared to SPA, which leads to a 3% increase in volume-

based reliability. In the near future and under a more critical scenario, considering the reduction in the runoff, the mean annual shortage has increased by about 18% in comparison with the baseline (GA-SPA), while the increasing deficit trend is more pronounced for the middle and far future periods. In terms of the vulnerability index, all three climate change periods under RCP2.6 and RCP8.5 scenarios show an increasing trend compared to the historical period. Under these conditions, the average vulnerability index in the near future period is close to 68% and in subsequent periods, this index has reached 72% and 70%, mainly due to reduced inflow into the reservoir.

Figure 8.

Table 6.

4.4.2. Static and Dynamic Hedging Rules as an Adaptive Policy

In this section, static and dynamic critical rule curves (S-CRC and D-CRC) were investigated as an adaptation strategy with climate change based on an optimized rule curve (Figure 9). In the case of S-CRC, $\alpha = 0.84$ is the rationing rate for all months and for D-CRC $\alpha = 0.52, 0.26, 0.87, 0.68, 0.5, 0.53, 0.77, 0.36, 0.37, 0.7, 0.59, 0.37$ per month. Then, reservoir performance indices were calculated for both of them. In the near, middle, and far future, the mean annual shortage with the static hedging rules is reduced by 56% compared to the no hedging (from 464 MCM to 204 MCM), which leads to a significant decrease (14%) in time-based reliability. In terms of the vulnerability index, all three climate change periods under RCP2.6 and RCP8.5 scenarios show a decreasing trend compared to no hedging. Under these conditions, the average vulnerability index in the near future period is close to 24% and in subsequent periods, this index has reached 33% and 29%, mainly due to reduced inflow into the reservoir. Compared to simulation using static hedging rules, dynamic hedging rules improved time-based reliability and vulnerability indices by 6% and 9%, respectively.

Figure 9.

5.Conclusions

This study aimed to analyze optimal rule curves with non-adaptive and adaptive policies for near, middle, and far future in the river basin of Zarrineh Rud. The SDSM model showed that large-scale variables including ncepp5_vgl, ncepp500gl, and ncepptempgl have the highest correlation with precipitation and temperature. The runoff simulations with HBV-Light showed that decreasing precipitation and increasing temperature would cause the reservoir inflow to decrease. Accordingly, the highest average annual runoff decrease was observed in the middle period for two scenarios. GA was used to optimize the decision variables including the lower and upper storage values for each month (LRC-GA-SPA,

URC-GA-SPA) through static rationing ratio (α) for all months and dynamic rationing ratio for each month of the year. The performance indices of the reservoir directly linked to water shortage, including time and volume-based reliability and vulnerability, were used to investigate the impact of adaptive policy. The results showed that the average vulnerability index with the adaptive policy was reduced significantly (by 60%) compared to the non-adaptive policy. Moreover, increasing the number of failure periods led to significant deterioration in the time-based reliability index. Finally, it can be said that the least and most significant effect of the adaptive policy is on the volume-based reliability and vulnerability index. In addition, static hedging rules improved the reservoir performance better than dynamic hedging rules.

Declarations

Availability of data and material: All data used in this article have been prepared from the Ministry of Energy and Meteorological Organization of Iran and after validation, have been used.

Code availability: The softwareused in this research will be available (by the corresponding author), upon reasonable request.

Ethics approval: Not applicable, because this article does not contain any studies with human or animal subjects.

Consent to participate: The data of this research were not prepared through a questionnaire.

Consent for publication :There is no conflict of interest regarding the publication of this article. The authors of the article make sure that every one agrees to submit the article and is aware of the submission.

Author's Contribution: M.M.: conceptualization, methodology, technical Investigation; S.A.: software, Validation; A.K.: writing- original draft preperation.

Funding: This research was funded by Agricultural Experiment station of Arak University, Iran.

Conflict of interest: The authors declare no conflict of interest.

References

1. Adeloye, A.J., M. Montaseri and C. Garman. 2001. Curing the misbehaviour of reservoir capacity statistics by controlling shortfall during failures using the modified sequent peak algorithm,Water Resour. Res., 37 (1), 73-82.
2. Abdi, R., M. Yasi., R. Sokooti Oskoui and E. Mohammadi. 2014. Environmental requirement assessment in Zarrinehrood River by hydrological methods. Journal of Watershed Engineering and management, 6(3):211-223 (In Presian).
3. Adeloye, A. and Q.V. Dau. 2019. Hedging as an adaptive measure for climate change induced water shortage at the Pong reservoir in the Indus Basin Beas River, India, Science of the Total Environment,687: 554-566.
4. Adeloye, A.J., B.S. Soundharajan, C. S. P. Ojha and R. Remesan. 2016. Effect of Hedging-Integrated Rule Curves on the Performance of the Pong Reservoir (India) During Scenario-Neutral Climate Change Perturbations. Journal of Water Resources, 30(2):445-470.
5. Adeloye, A.J., N.R. Nawaz, T.J. Bellerby. 2013. Modelling the impact of climate change on water systems and implications for decision makers. Chapter 11. In: Surampali, R.Y.,et al. (Eds.), Climate Change Modelling, Mitigation, and Adaptation. Environmental & Water Resources Institute, ASCE, pp. 299–326.
6. Ahmadzadeh, H., S. Morid, M. Delavar and R. Srinivasan. 2016. Using the SWAT model to assess the impacts of changing irrigation from surface to pressurized systems on water productivity and water saving in the Zarrineh Rud catchment. Agricultural Water Management, 175: 15-28.
7. Alimohammadi, H., A.Massah Bavani, and A.Roozbahani. 2020. Mitigating the Impacts of Climate Change on the Performance of Multi-Purpose Reservoirsby Changing the Operation Policy from SOP to MLDR, Water Resources Management, 34, 1495–1516.
8. Anvari, S., SJ. Mousavi, S. Morid. 2017. Stochastic dynamic programming-based approach for optimal irrigation scheduling under restricted water availability conditions. Irrigation and Drainage, 66(4), 492-500.
9. Anvari, S., JH. Kim, M.Moghaddasi. 2019. The role of meteorological and hydrological uncertainties in the performance of optimal water allocation approaches. Irrigation and Drainage. 68(2), 342-353.
10. Ashofteh, P. and O.Bozorg Hadad. 2015. Extracting rule curve of the reservoir under climate change, Soil and Water Reserch, 45(2), 113-121, (In Presian).
11. Bhatia, N., R. Srivastav and K. Srinivasan. 2018. Season-dependent hedging policies for reservoir operation – a comparison study. Water 10 (10), 1311.
12. Bergström, S., 1976. Development and application of a conceptual runoff model for Scandinavian catchments, Bulletin Series A, No. 52 – SMHI report RH07, Norrköping: Swedish Meteorological and Hydrological Institute, 134.
13. Bergström, S., 1995. The HBV model. In: V.P. Singh, ed. Computer models of watershed hydrology. Highlands Ranch, CO: Water Resources Publication, 443–476.

14. Castillo, O., P. Melin, W. Pedrycz and J. Kacprzyk. 2014. Recent advances on hybrid approaches for designing intelligent systems, Part of the Studies in Computational Intelligence book series (SCI, volume 547), Springer. Tijuana, Mexico.
15. Chang, J., A.Gue, Y.Wang , Y.Ha, R. Zhang, L. Xue and Z. Tu. 2019. Reservoir operations to mitigate drought effects with a hedging policy triggered by the drought prevention limiting water level. Water Resour. Res. 55, 904–922.
16. Chen L., J. Mcphee, and W.W.G. Yeh. 2007. A diversified multi-objective GA for optimizing reservoir rule curves. Journal of Advances in Water Resources, 30(5): 1082–1093.
17. Compos J.N.B. 2010. Modeling the yield–evaporation–spill in the reservoir storage process: The regulation triangle diagram. Journal of Water Resources Management, 24: 3487–3511.
18. Demirel, MC., MJ. Booij, and AY. Hoekstra.2013. Effect of different uncertainty sources on the skill of 10 day ensemble low flow forecasts for two hydrological models. Water resources research, 49(7), 4035-4053.
19. Ehteram, M., S.F. Mousavi, H. Karami, S. Farzin, V.P. Singh, K.-W. Chau, et al. (2018). Reservoir operation based on evolutionary algorithms and multi-criteria decision-making under climate change and uncertainty, J Hydroinformatics, 20(2), 332-355.
20. Eum, H., Y. Kim and R. Palmer. 2011. Optimal drought management using sampling stochastic dynamic programming with a hedging rule. J. Water Resour. Plan. Manag. 137 (1), 113–122.
21. Fowler, H.J., C.G.Kilsby and P.E.O'Connell. 2003. Modeling the impacts of climatic change and variability on the reliability, resilience and vulnerability of a water resource system. Water Resources Research, 39(8).
22. Goldberg, D. 1998. Genetic algorithm in search, optimization and machine learning, Addison Wesley publishing compane Inc, 401. Boston, United States.
23. Guo, S.L., H.G. Zhang and H.Chen. 2004. A reservoir flood forecasting and control System for China. Journal of Hydrological Sciences, 49(6): 959-972.
24. Hashimoto, T., J.R. Stedinger and D. P. Loucks .1982. Reliability, resiliency, and vulnerability criteria for water-resource system performance evaluation. Water Resources Management. 18:14–20.
25. Hernández-Bedolla, J., A. Solera, J. Paredes-Arquiola, M. Pedro-Monzonís, J. Andreu, S. 2017. Sánchez-Quispe The assessment of sustainability indexes and climate change impacts on integrated water resource management, Water, 9(3), 213.
26. IPCC, 2007. Summary for policymakers. Climate change 2007: the physical science basis. Contribution of the Working Group I to the Fourth Assessment Report of the Intergovernmental Panel on Climate Change. Cambridge University.
27. Jain, S. K .2010. Investigating the behavior of statistical indices for performance assessment of a reservoir. Journal of Hydrology. 391:90–96.
28. Kacprzyk, J. 2006. Studies in computational intelligence. Polish Academy of Sciences, Warsaw, Poland.

29. Kermani, A. H., H. Babazadeh, J. Porhemmat and M. Sarai-Tabrizi. 2020. An uncertainty assessment of reservoir system performance indices under the climate change effect, Ain Shams Engineering Journal, 11(4), 889-904.
30. Kia, E. 2018. The Impact of climate change on the reliability of water supply downstream of Haraz Dam, Ph.D. degree, Sari Agricultural Sciences and Natural Resources University.
31. Li, L., H. Xu, X. Chen. 2009. Streamflow forecast and reservoir operation performance assessment under climate change. Water resources management, 24(1), 83-104.
32. McMahon T.A. and A.J. Adeloye. 2005. Water Resources Yield, Water Resources Publications, Littleton, CO, USA.
33. Moghaddasi, M., S. Araghinejad and S.Morid. 2010. Long-term operation of irrigation dams considering variable demands: Case study of Zayandeh-rud reservoir, Iran. Journal of irrigation and drainage engineering, 136(5), 309-316.
34. Mushtaq, S. and M. Moghaddasi .2011. Evaluating the potentials of deficit irrigation as an adaptive response to climate change and environmental demand. Environmental science & policy, 14(8), 1139-1150.
35. Nawaz, N. R. and A. J. Adeloye. 2006. Monte Carlo assessment of sampling uncertainty of climate change impacts on water resources yield in Yorkshire, England. Climatic Change, 78(2), 257-292.
36. Pretto, P.B., F.H.S. Chiew, T.A. McMahon, R.M. Vogel, J.R. Stedinger.1997. The (mis)behavior of behavior analysis storage estimates, Water Resources Research, 33(4), 703-709.
37. Prasanchum, H. and A. Kangrang .2017. Optimal reservoir rule curves under climatic and land use changes for Lampao Dam using Genetic Algorithm. KSCE Journal of Civil Engineering, 22(1): 351–364.
38. Raje, D. and P.Mujumdar. 2010. Reservoir performance under uncertainty in hydrologic impacts of climate change. Journal of Advances in Water Resources, 33(3): 312-326.
39. Ripple, W. 1883. Capacity of storage reservoirs for water supply, In Minutes of the Proceedings of the Institution of Civil Engineers. Thomas Telford-ICE Virtual Library, 71, 270-278.
40. Sandoval-Solis, S, D.McKinney and D. Loucks. 2011. Sustainability index for water resources planning and management. Journal of Water Resources Planning and Management. 137:381–390.
41. Seibert, J. 1997. Estimation of parameter uncertainty in the HBV model. Nordic Hydrology, 28 (4/5), 247–262.
42. Seibert, J. 2000. Multi-criteria calibration of a conceptual runoff model using a genetic algorithm, Hydrology and Earth System Sciences, 4(2), 215-224.
43. Seibert, J. and M.J.P. Vis. 2012. Teaching hydrological modeling with a user-friendly catchment-runoff-model software package. Hydrology and Earth System Sciences, 16(9), 3315-3325.
44. Soundharajan, B. S., A.J. Adeloye and R. Remesan .2016. Evaluating the variability in surface water reservoir planning characteristics during climate change impacts assessment. Journal of Hydrology, 538 (10): 625–639.

45. Srinivasan, K. and K. Kumar. 2018. Multi-objective simulation-optimization model for longterm reservoir operation using piecewise linear hedging rule. Water Resour. Manag. 32 (2), 1901–1911.
46. Traynham, L., R. Palmer, A. Polebitski. 2011. Impacts of future climate conditions and forecasted population growth on water supply systems in the puget sound region J Water Resour Plann Manage, 137 (4) , 318-326.
47. Tu, M.Y., Hsu, N.S., Tsai, F.T.C., Yeh, W.W.G., 2008. Optimization of hedging rules for reservoir operations. J. Water Resour. Plan. Manag. 134 (1), 3–13.
48. Wilby, R. L., C. W. Dawson, and E. M. Barrow. 2002. SDSM a decision support tool for the assessment of regional climate change impacts. Environmental Modelling and Software, 17(2), 145-157.
49. Yeh, J. Y. and W. S. Lin. 2007. Using simulation technique and genetic algorithm to improve the quality care of a hospital emergency department, Expert Systems with Applications, 32(4), 1073-1083.
50. Yin, X. A., X. F. Mao, B. Z. Pan and Y.W. Zhao. 2015. Suitable range of reservoir storage capacities for environmental flow provision. Ecological Engineering, 76, 122-129.

Figures

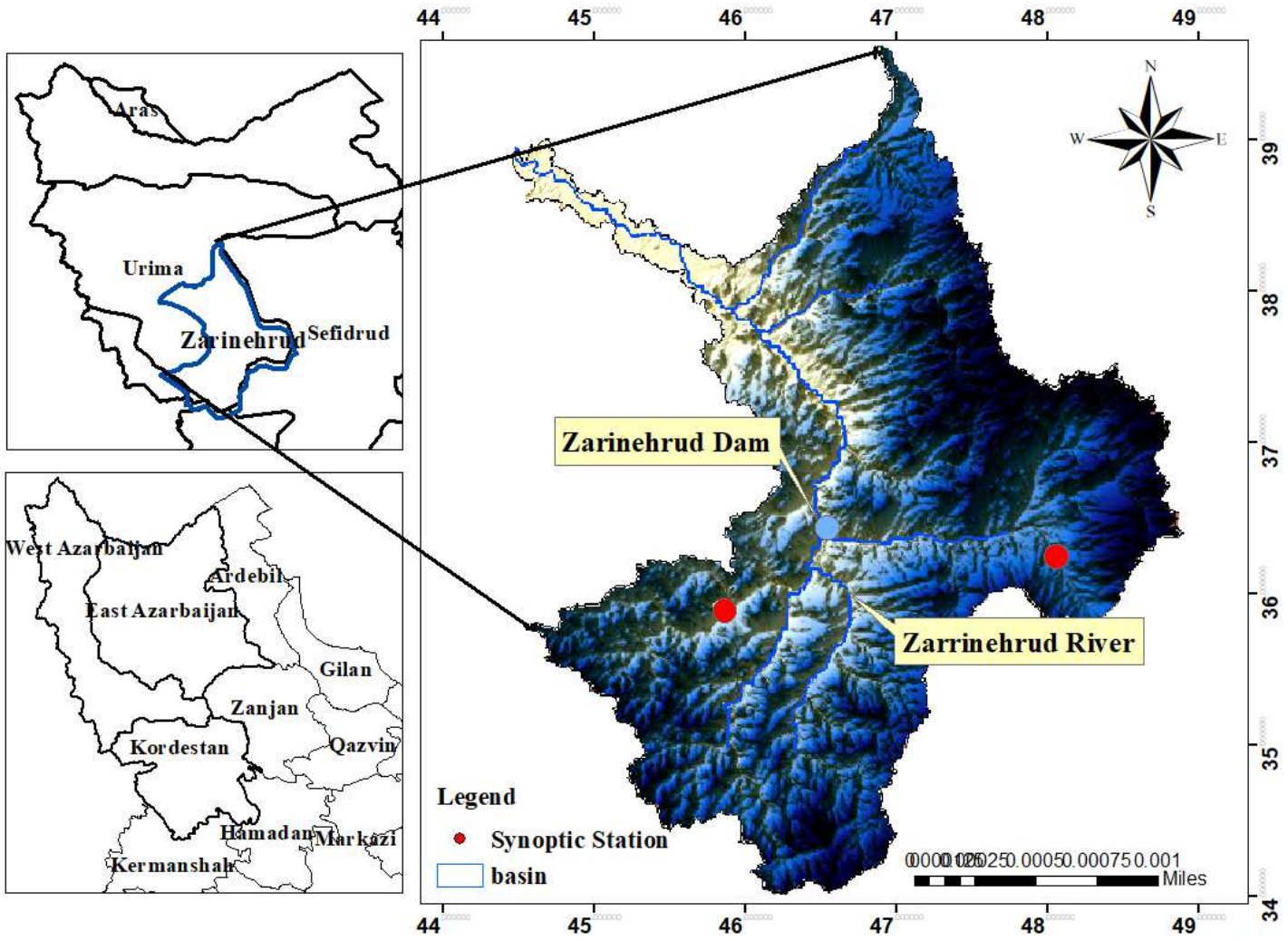

Figure 1

The Case study Note: The designations employed and the presentation of the material on this map do not imply the expression of any opinion whatsoever on the part of Research Square concerning the legal status of any country, territory, city or area or of its authorities, or concerning the delimitation of its frontiers or boundaries. This map has been provided by the authors.

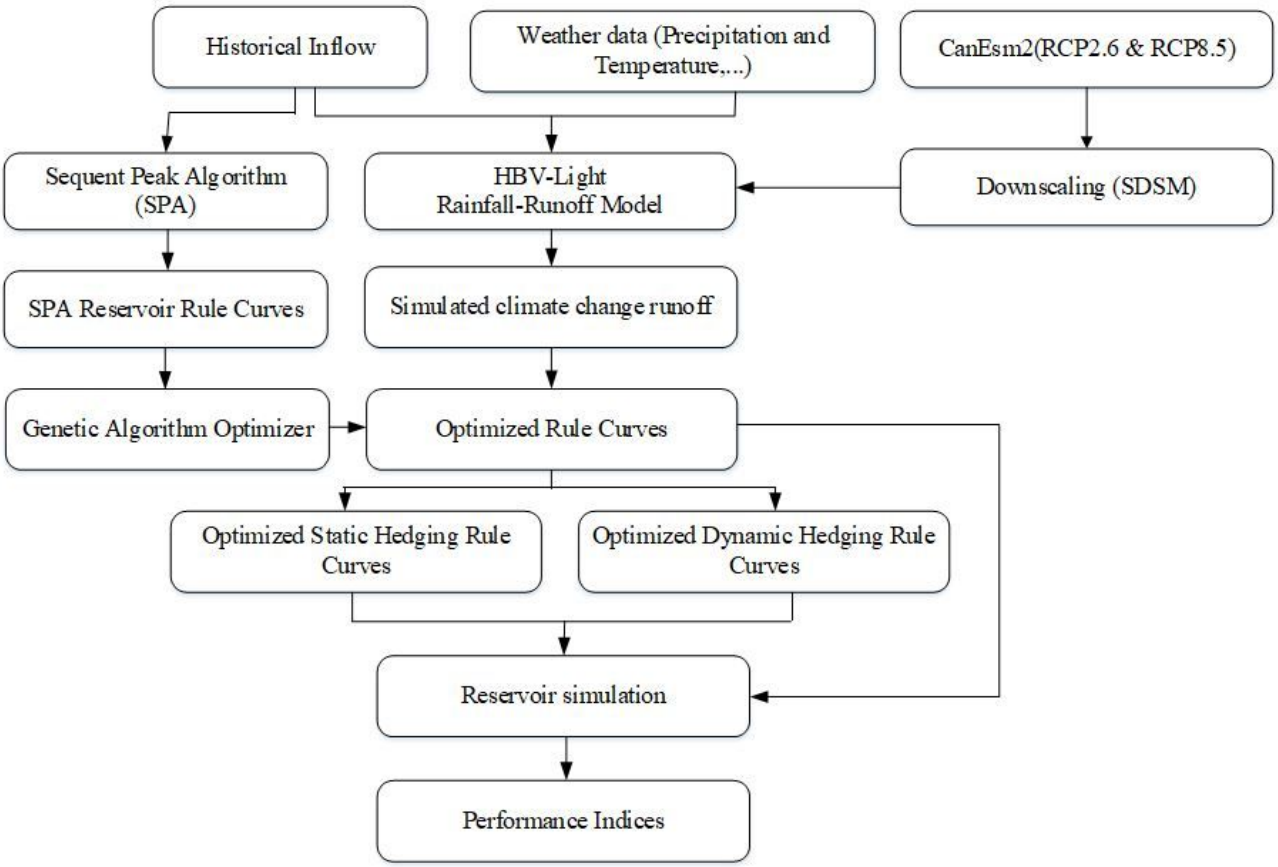

Figure 2

The research flowchart

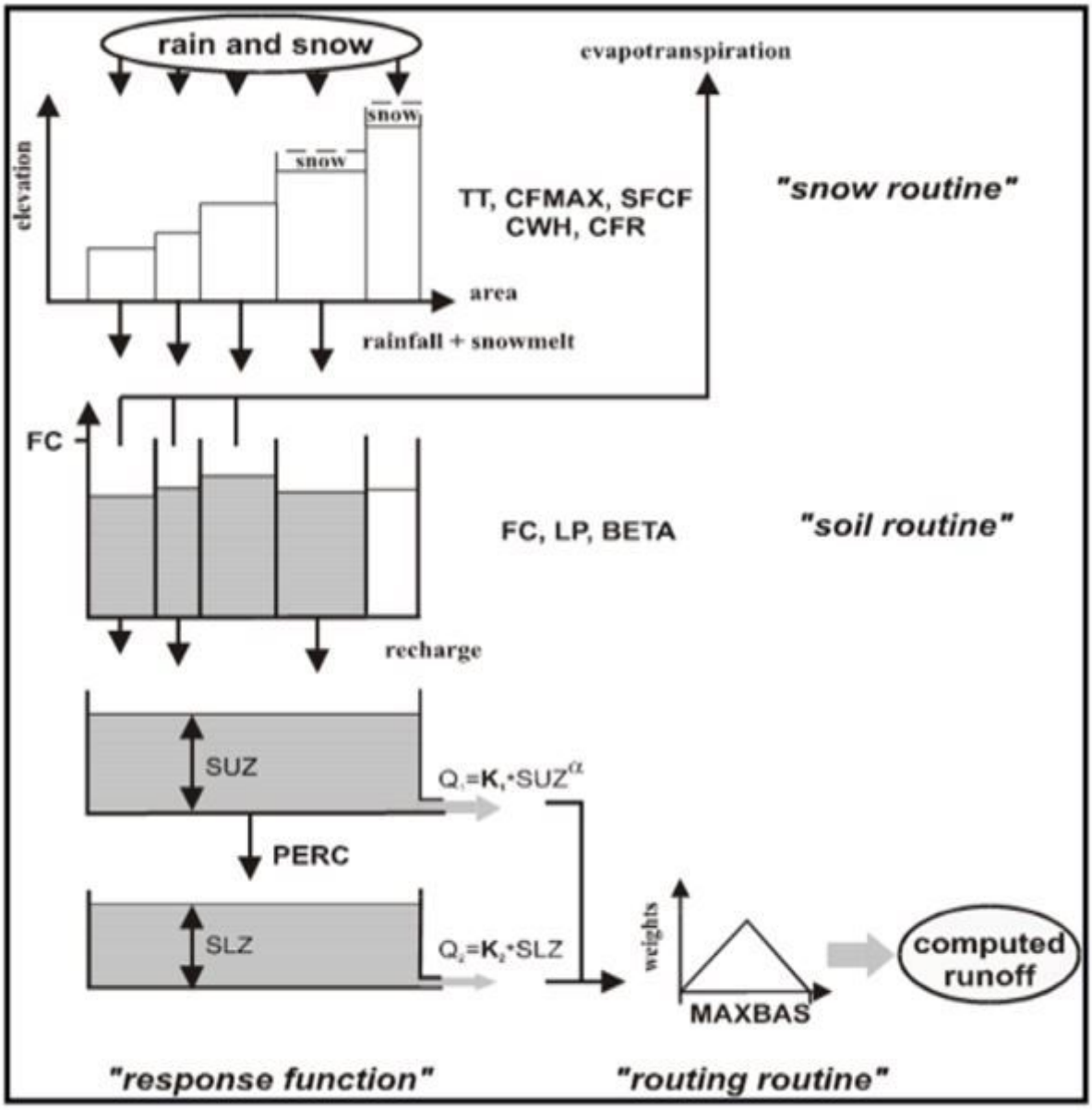

Figure 3

The structure of HBV-light model (Seibert, 2000)

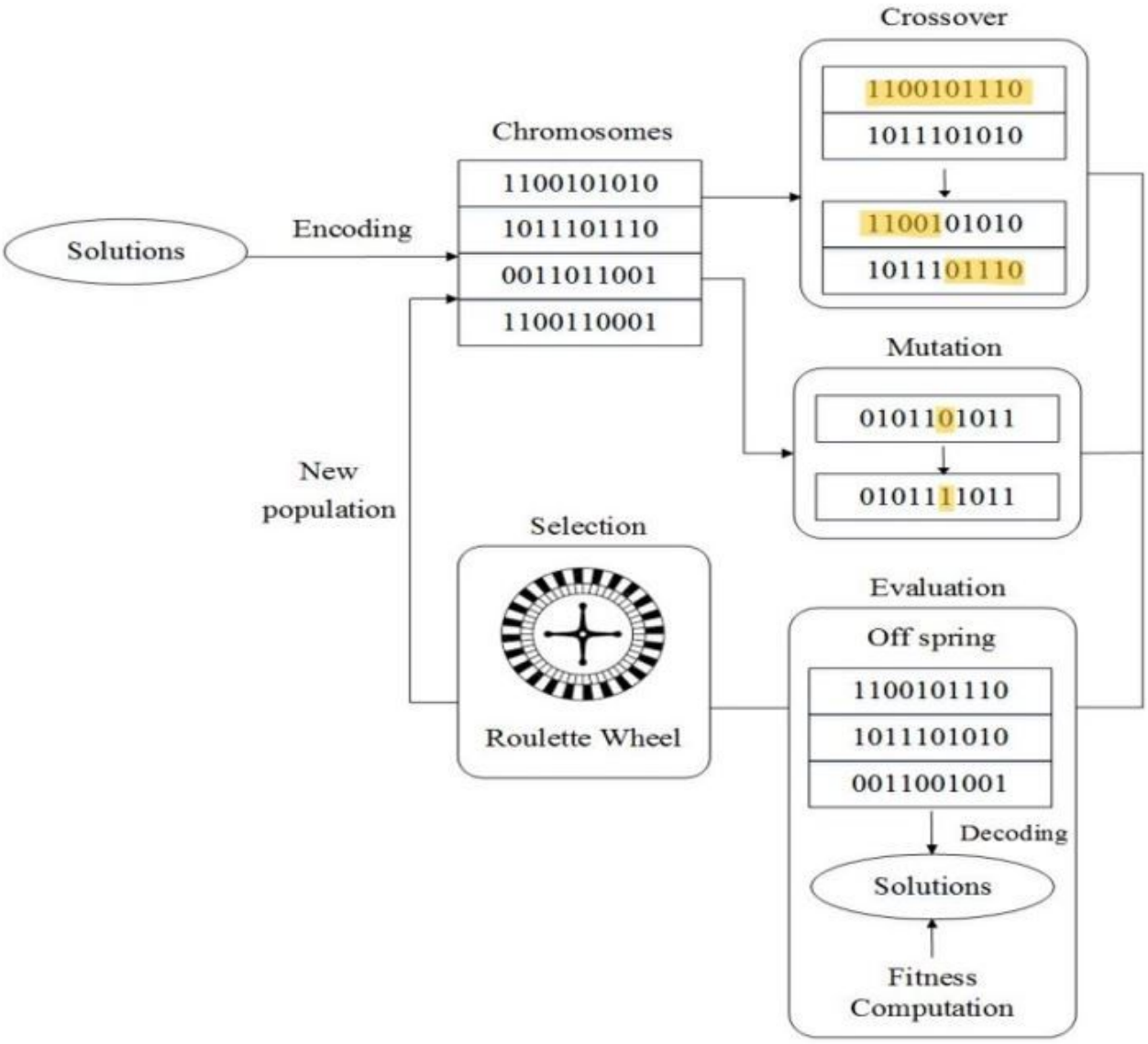

Figure 4

Flowchart of computational stages in GA (Adopted from Yeh & Lin, 2007)

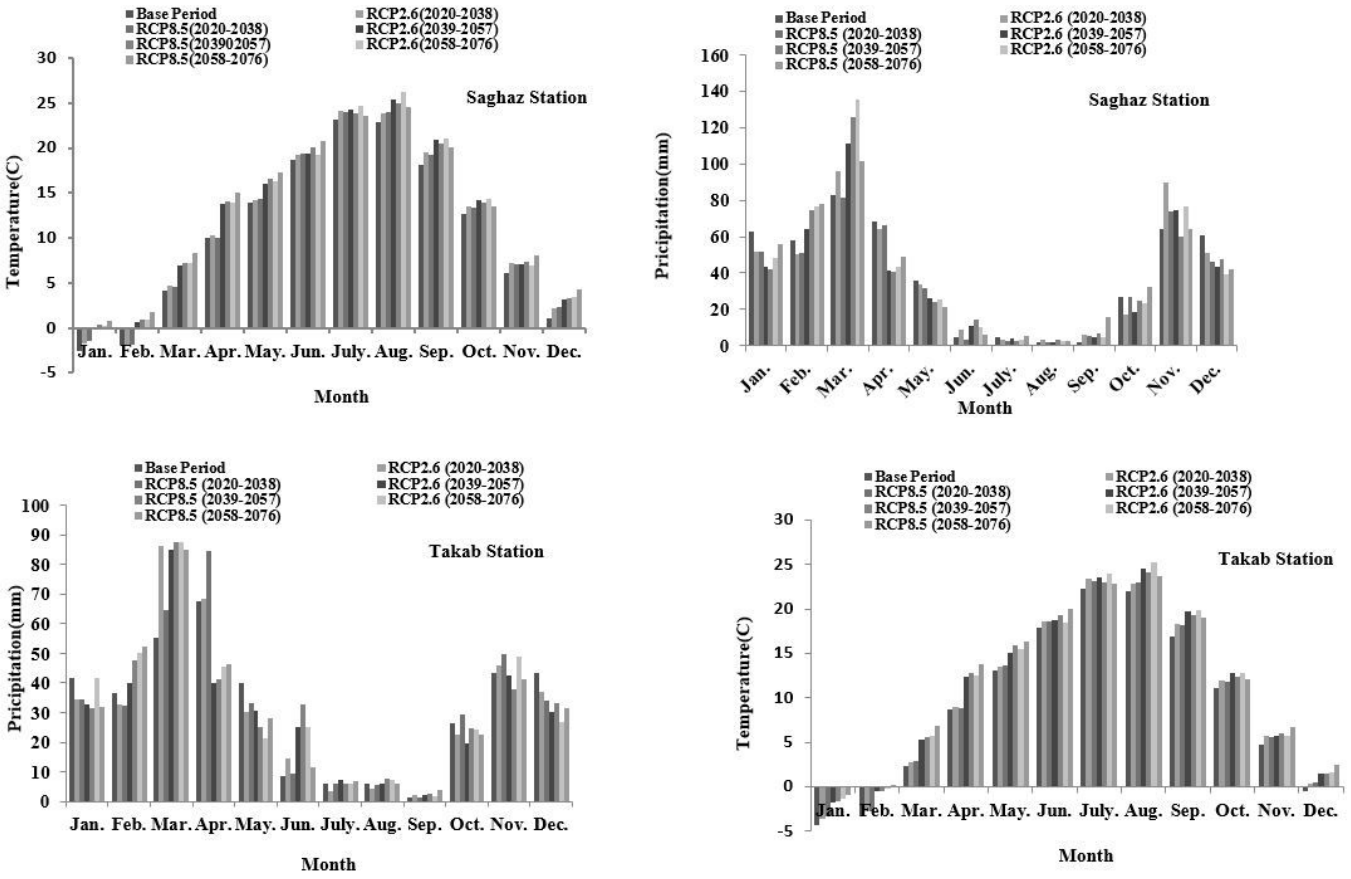

Figure 5

Changes of monthly mean temperature and precipitation in the near, middle, and far future compared to the baseline for RCP2.6 and RCP8.5 scenarios (Saghaz and Takab stations)

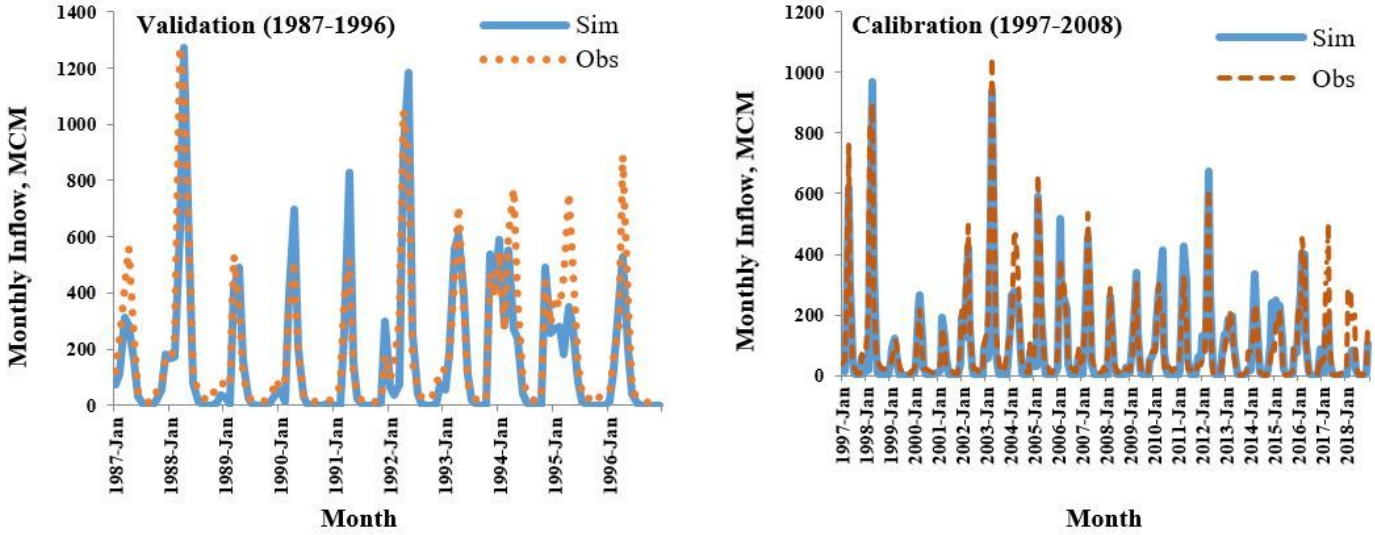

Figure 6

Comparison of observed and simulated monthly river flow during calibration and validation

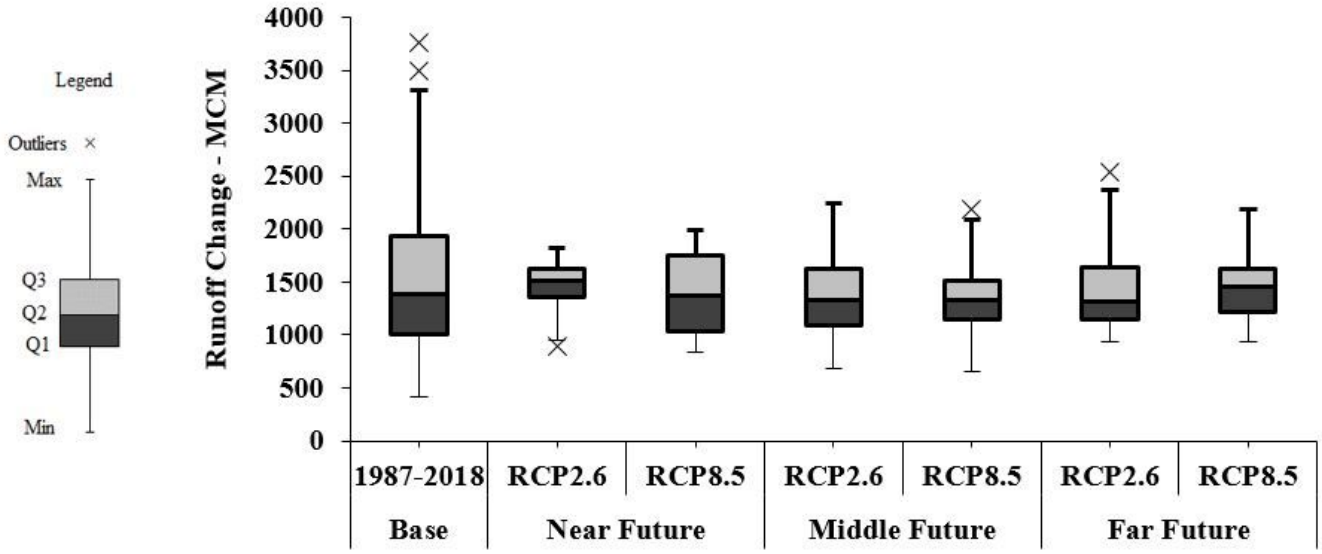

Figure 7

Changes of runoff in the baseline and near, middle, and far future (Q1=Mean, Q2=25%, Q3=75%)

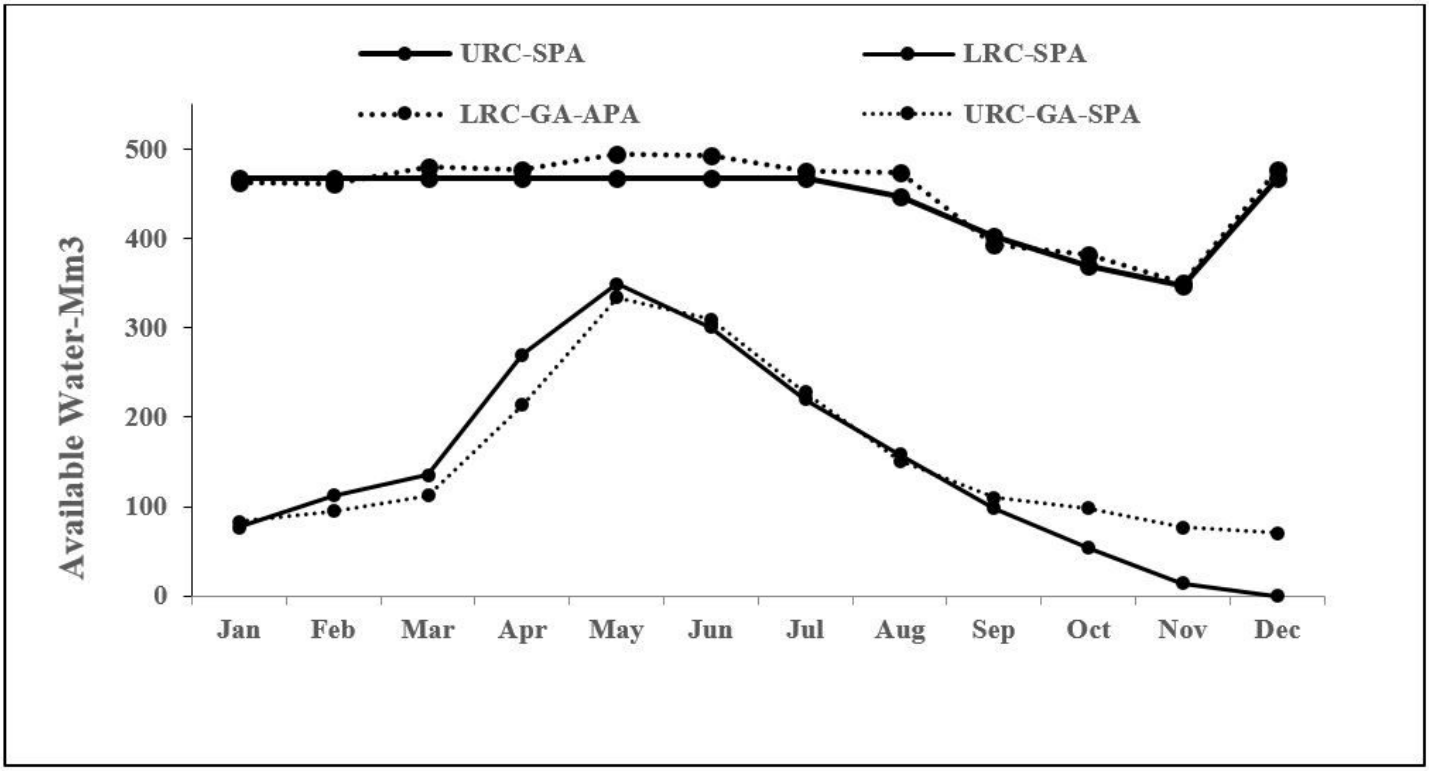

Figure 8

Rule curves developed by coupled SPA-GA optimization

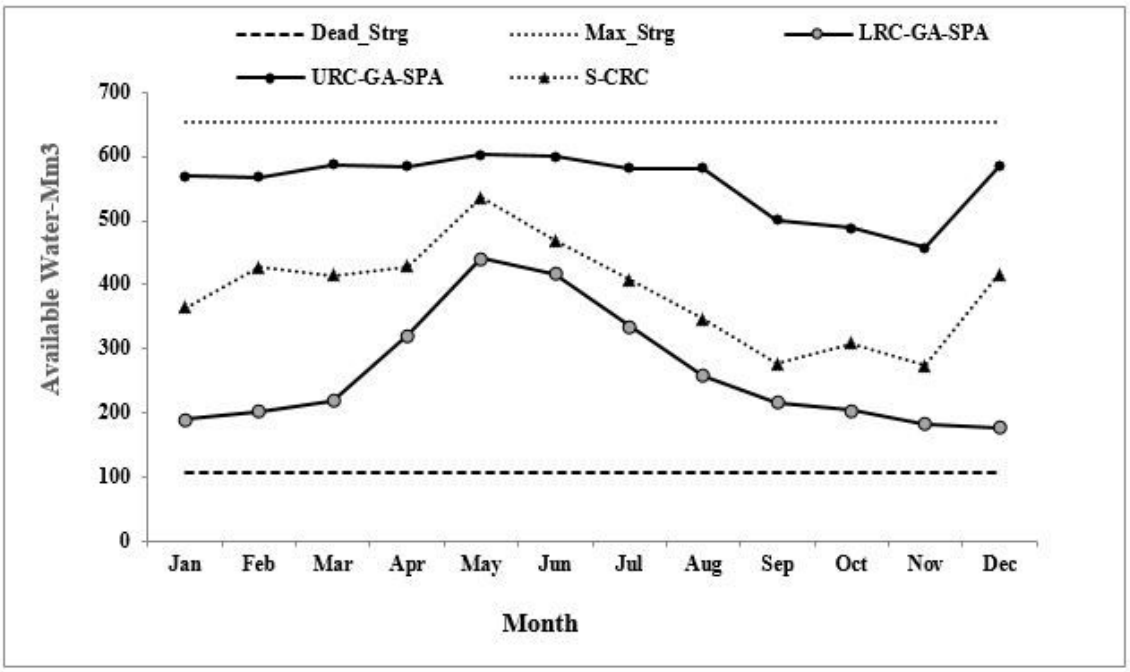

a

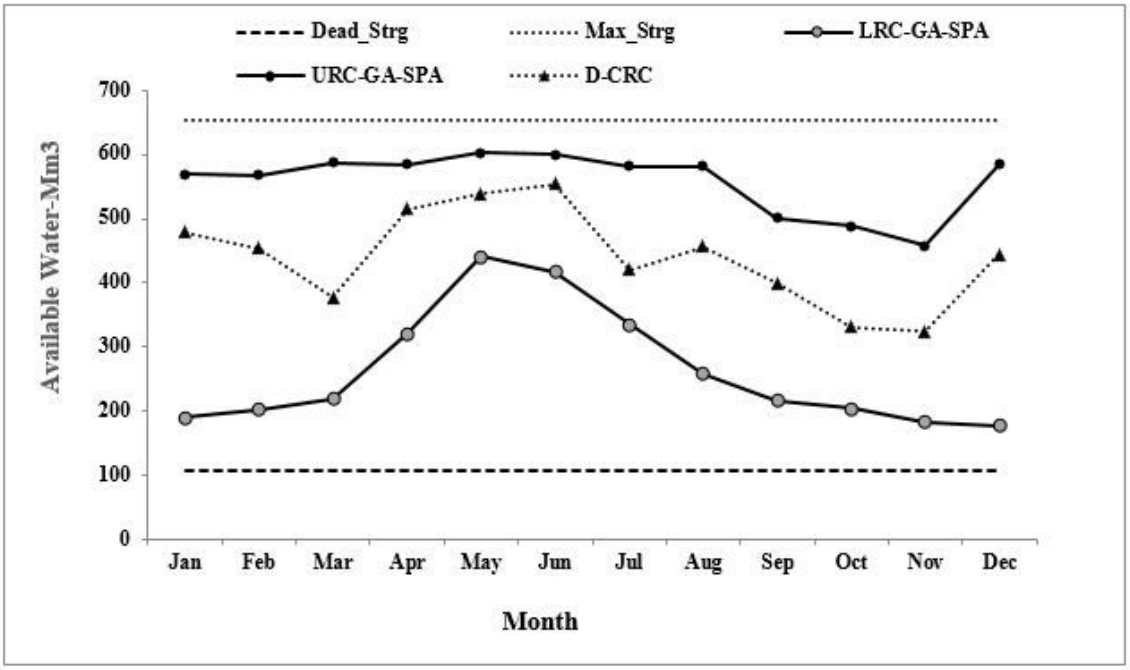

b

Figure 9

Rule curves developed by coupled SPA-GA optimization under static(a) and dynamic (b) hedging rules

Supplementary Files

This is a list of supplementary files associated with this preprint. Click to download.

- Table1.jpg